Structure of phase III of solid hydrogen

Supplementary information

Chris J. Pickard[1] & Richard J. Needs[2]

[1]*Scottish Universities Physics Alliance, School of Physics and Astronomy, University of St Andrews, St Andrews, Fife, KY16 9SS, United Kingdom*
[2]*Theory of Condensed Matter Group, Cavendish Laboratory, Cambridge CB3 0HE, United Kingdom*

1 Supplementary Methods

The search procedure We used a slightly modified version of the procedure described in Ref. 1, in that no restrictions were placed on the cell vectors or angles, save a constraint that the volume was scaled randomly to within 0.5 and 1.5 of a reasonable value.

Details of the searches Very extensive searches were performed with both 8 and 12-atom unit cells, which implicitly includes searches over smaller cells of 1, 2, 3, 4, and 6 atoms. In the 8 and 12-atom searches, the relaxed structures with low enthalpies were generated several times, indicating that these searches are nearly exhaustive. We also performed searches at 100 GPa using 16 and 24-atom unit cells, and at 200 GPa using 24 and 48 atom unit cells, and at 300 GPa using 10, 14, 16, and 18-atom unit cells. The 48-atom search was certainly not exhaustive.

Because our searches over the smaller cells of 12 and less atoms are, we believe, essentially exhaustive, we can say that it is not likely that other structures with similar or lower DFT enthalpies will be found with 12 or less atoms per cell. We cannot, of course, rule out the possibility that structures with larger cells might be more stable.

Details of the DFT calculations We used a developer's version of the CASTEP code[2]. The Perdew-Burke-Ernzerhof (PBE) Generalised Gradient Approximation (GGA) density functional[3] was used. For the initial search over structures we used default ultrasoft pseudopotentials[4]. The k-point sets were generated separately for each unit cell encountered during the procedure, and no symmetry restrictions were applied. A medium quality Brillouin zone sampling, consisting of a grid of spacing $2\pi\times$ 0.07 Å^{-1}, and a plane wave basis set cutoff of 340 eV were found to be sufficient for the initial search over structures. When re-calculating the enthalpy curves with higher accuracy, we used a Brillouin zone sampling of $2\pi\times$ 0.04 Å^{-1}, more accurate pseudopotentials and a plane wave cutoff of 500 eV.

We neglected the ZP motion of the protons during the search, but subsequently estimated its impact

on the relative stabilities using harmonic ZP energy calculations. Γ-point phonon frequencies were calculated in super-cells containing 96 (64 for $Pa3$ and 128 for $P6_3/m$) atoms using a finite difference approach at various volumes, with Brillouin zone sampling of $2\pi\times$ 0.05 Å^{-1}, more accurate pseudopotentials, a cutoff energy of 300 eV, and a very dense augmentation charge grid, which is required for the finite-difference calculations. The ZP energies were estimated as $1/2\,\hbar\bar{\omega}$, where $\bar{\omega}$ is the average phonon frequency over the Brillouin zone. The ZP energies were fitted to quadratic polynomials in the volume, and the ZP enthalpies were determined from the fits.

The IR activities of the zone centre vibrational modes were calculated using density functional perturbation theory[5]. The Coulomb potential was used for the proton instead of a pseudopotential. A Brillouin zone sampling grid with $2\pi\times$ 0.05 Å^{-1} was used, with a plane wave basis set cutoff of 960 eV. The structures were fully relaxed at this level of accuracy for each pressure.

2 Supplementary Results and Discussion

Sensitivity to the density functional To gain some insight into the sensitivity of our results to the choice of exchange-correlation density functional, we repeated some of the calculations using the Local Density Approximation (LDA) functional. The results were similar to those obtained with the PBE-GGA functional, a typical example being that the coexistence pressure for $Pca2_1$ and $Cmca$ is predicted to be about 185 GPa using PBE-GGA, and 135 GPa with the LDA.

Stability of the structures to elastic and phonon distortions Because our structures are generated by enthalpy minimisation without symmetry constraints, they are stable to elastic distortions and to optical phonon displacements at the zone centre of the unit cell generated by the search procedure. To determine the ZP energies, we calculated the phonons at the zone centres of larger super-cells, see Section 1, for the $Pa3$, $Pca2_1$, $P2_1/c$, $P6_3/m$, $C2/c$, $Cmca$-12, $C2$, $Pbcn$, and $Cmca$ phases. In some cases we encountered imaginary phonon frequencies, indicating that the enthalpy may be lowered by a phonon distortion. We can quantify the degree of instability by averaging the moduli of the imaginary frequencies over the Brillouin zone. At 100 GPa this procedure gave 6 meV per proton for $Cmca$, which is a rather unstable structure, about 1 meV per proton for $Pbcn$ and $P2_1c$, and numbers an order of magnitude or more smaller for the other structures, indicating that they are very nearly stable to phonon distortions at this pressure.

On calculating the zone centre vibrational modes of $P6_3/m$ it was found that the frequency of the lowest libron became unstable above 125 GPa. On following this mode, $P6_3/m$ relaxed to the $P2_1/c$ structure.

Stability of atomic structures Our results indicate that atomic structures would become stable at about 500 GPa at the static lattice level of theory, in contradiction to the conclusion of Oganov and Glass[6] that hydrogen retains its molecular structure even at 600 GPa.

Discovery of $Pbcn$ and the "mixed" structures $Ibam$ was not obtained in the lower-pressure searches, and calculations at 200 GPa revealed it to have an unstable phonon mode commensurate with a super-cell containing 48 atoms. We made small atomic displacements to the $Ibam$ structure in the 48 atom cell and performed a full relaxation. The resulting orthorhombic structure of space group $Pbcn$ is illustrated in detail in Figs. 1 and 2. The $Pbcn$ mixed structure is competitive over a wide range of pressures. The $C2$ phase, which is very competitive around 100 GPa, is similar to $Pbcn$, except that the less strongly bonded layer is a compressed version of that of the $C2/c$ structure. At pressures above 300 GPa, the less strongly bonded layers in these structures are best described as "atomic". On compression above 350 GPa, both $C2$ and $Pbcn$ evolve continuously into the higher symmetry $Ibam$ structure, which consists of alternating hexagonal atomic graphene-like sheets and layers of molecular hydrogen forming a herring-bone pattern.

The mixed structures represent a more gradual route from molecular to atomic phases which allows the retention of high vibronic frequencies to elevated pressures. If such mixed structures were to occur, they might show interesting isotopic effects such as the segregation of deuterium and protium between the molecular and atomic layers.

Stability at higher pressures including ZP vibrational effects The enthalpies including ZP vibrational effects at the harmonic level of the most competitive phases are shown in Fig. 3. The $Cmca$-12 structure is more stable than $C2/c$ above about 240 GPa. The $Pbcn$ "mixed" structure is very competitive in the region of the transition.

Vibrational modes of the $Pca2_1$, $P6_3/m$, $Cmca$-12, and $C2/c$ structures The variation with pressure of the vibrational frequencies of the $Pca2_1$, $P6_3/m$, $Cmca$-12, and $C2/c$ structures is shown in Fig. 4, while their simulated IR spectra at 150 GPa are shown in Fig. 5. The simulated IR spectra of Fig. 5 illustrate the weak IR activity of $Pca2_1$, $P6_3/m$, and $Cmca$-12, compared with that of $C2/c$.

The vibron modes are separated from the lower frequency modes by a large gap. In general, the vibron modes soften with increasing pressure. $Pca2_1$ has three low-intensity IR active modes. $P6_3/m$ has a single medium intensity IR active vibron mode whose frequency varies very little with pressure. $Cmca$-12 has two medium intensity IR active vibron modes. $C2/c$ has six IR active vibron modes, three of which are of low intensity, while the other three are close in frequency and form a single very strong IR vibron peak at about 4100 cm^{-1} in Fig. 5. The libron/phonon modes mostly harden with increasing pressure, although the instability in the lowest libron mode of $P6_3/m$ at about 125 GPa is clearly visible.

The pressure dependencies of the libron modes of $C2/c$ are compared with experimental data for the Raman active libron modes in Fig. 6. The calculated libron modes gently increase with pressure in a similar fashion to experiment. In detail the agreement is not precise, but considering the use of an approximate density functional (which often gives large fractional errors in low frequency

vibrational modes), and the neglect of the pressure arising from vibrational effects, and anharmonic and finite temperature effects, the agreement is quite satisfactory.

1. Pickard, C. J. & Needs, R. J. High pressure phases of silane. *Phys. Rev. Lett.* **97**, 045504 (2006).

2. Clark, S. J. *et al*. First principles methods using CASTEP. *Z. Kristallogr.* **220**, 567–570 (2005).

3. Perdew, J. P., Burke, K. & Ernzerhof, M. Generalized gradient approximation made simple. *Phys. Rev. Lett.* **77**, 3865–3868 (1996).

4. Vanderbilt, D. Soft self-consistent pseudopotentials in a generalized eigenvalue formalism. *Phys. Rev. B* **41**, 7892–7895 (1990).

5. Refson, K., Tulip, P. R. & Clark, S. J. Variational density functional perturbation theory for dielectrics and lattice dynamics. *Phys. Rev. B* **73**, 155114 (2006).

6. Oganov A. R. & Glass, C. W. Crystal structure prediction using ab initio evolutionary techniques: Principles and applications. *J. Chem. Phys.* **124**, 244704 (2006).

7. Goncharov, A. F., Gregoryanz, E., Hemley, R. J. & Mao, H.-K. Spectroscopic studies of the vibrational and electronic properties of solid hydrogen to 285 GPa. *Proc. Natl Acad. Sci. USA* **98**, 14234–14237 (2001).

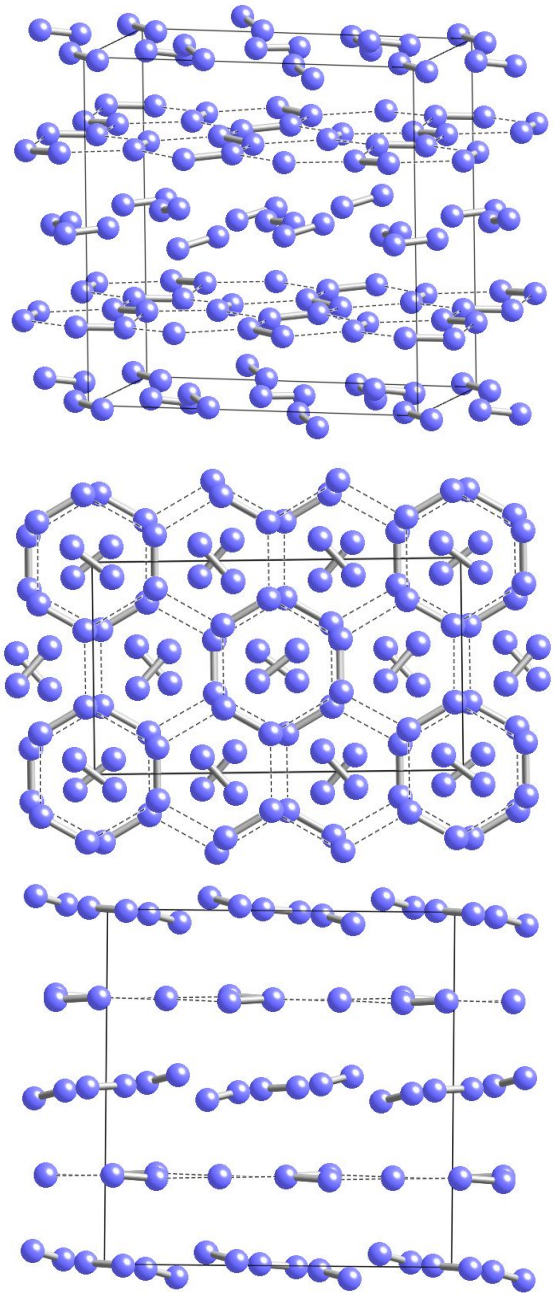

Figure 1: **The $Pbcn$ structure at 150 GPa.** The dashed lines denote contacts between 0.8 Å and 1.35 Å and the solid lines those less than 0.8 Å.

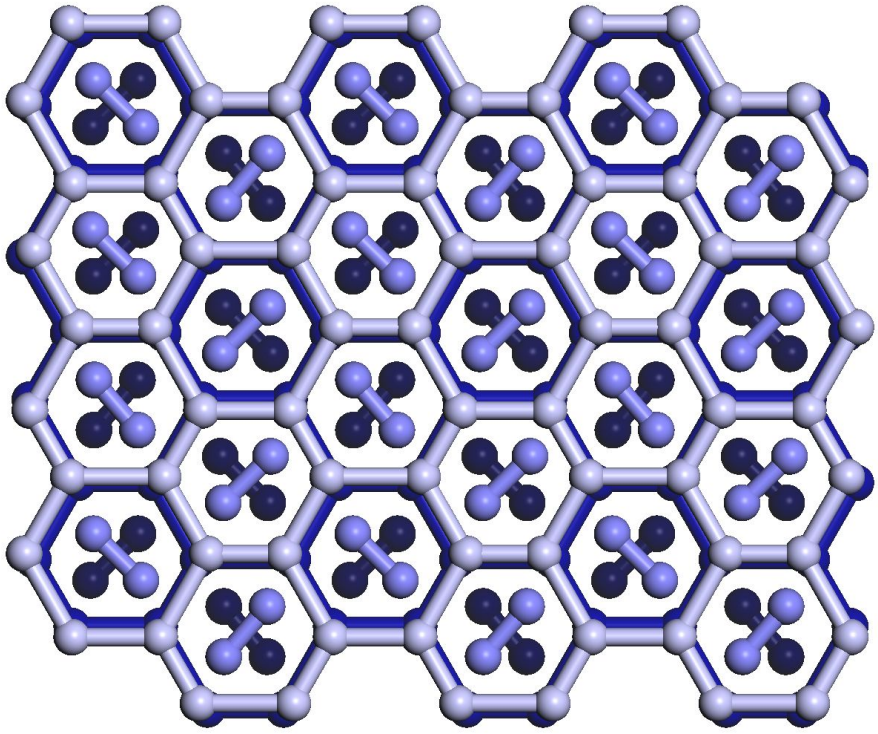

Figure 2: **The $Pbcn$ structure at 300 GPa.** Four layers are depicted, with the colour become successively darker for each deeper layer. On applying further pressure, the bond lengths within the less strongly bonded graphene-like layers become more nearly equal, and the $Ibam$ structure is formed.

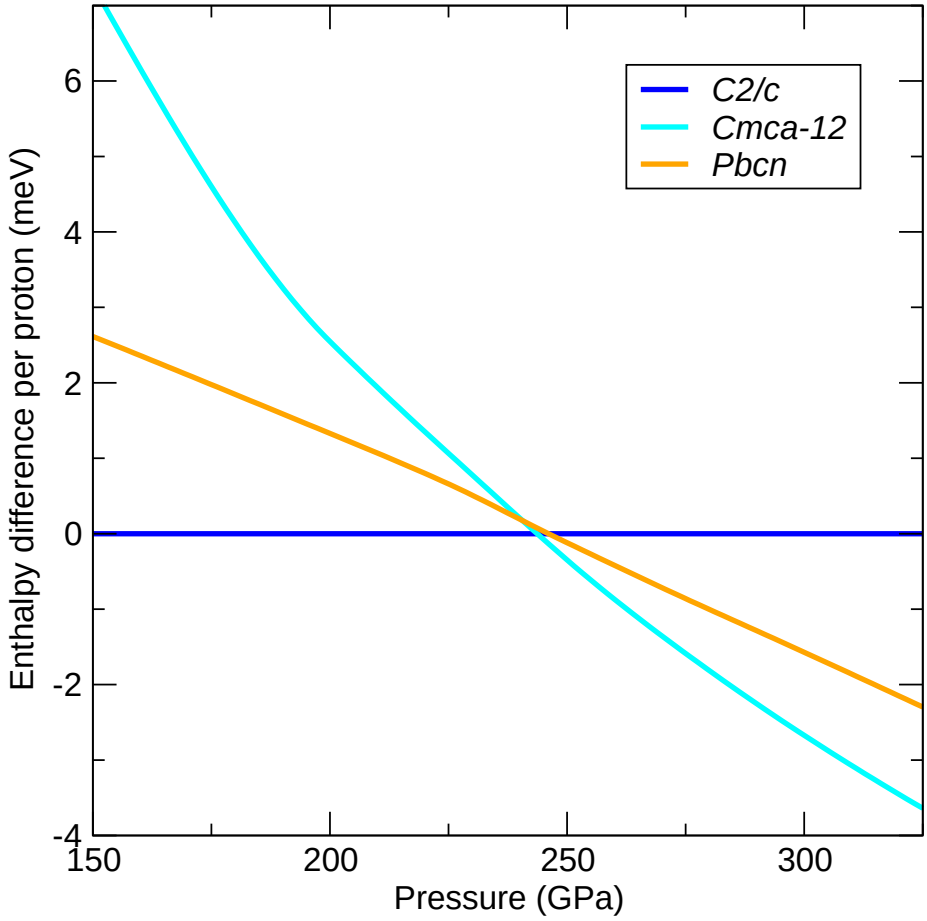

Figure 3: **Enthalpy plot for higher pressures.** The enthalpies, including ZP vibrational effects at the harmonic level, for the $C2/c$, $Pbcn$, and $Cmca$-12 structures. Note the large pressure range, and small enthalpy differences.

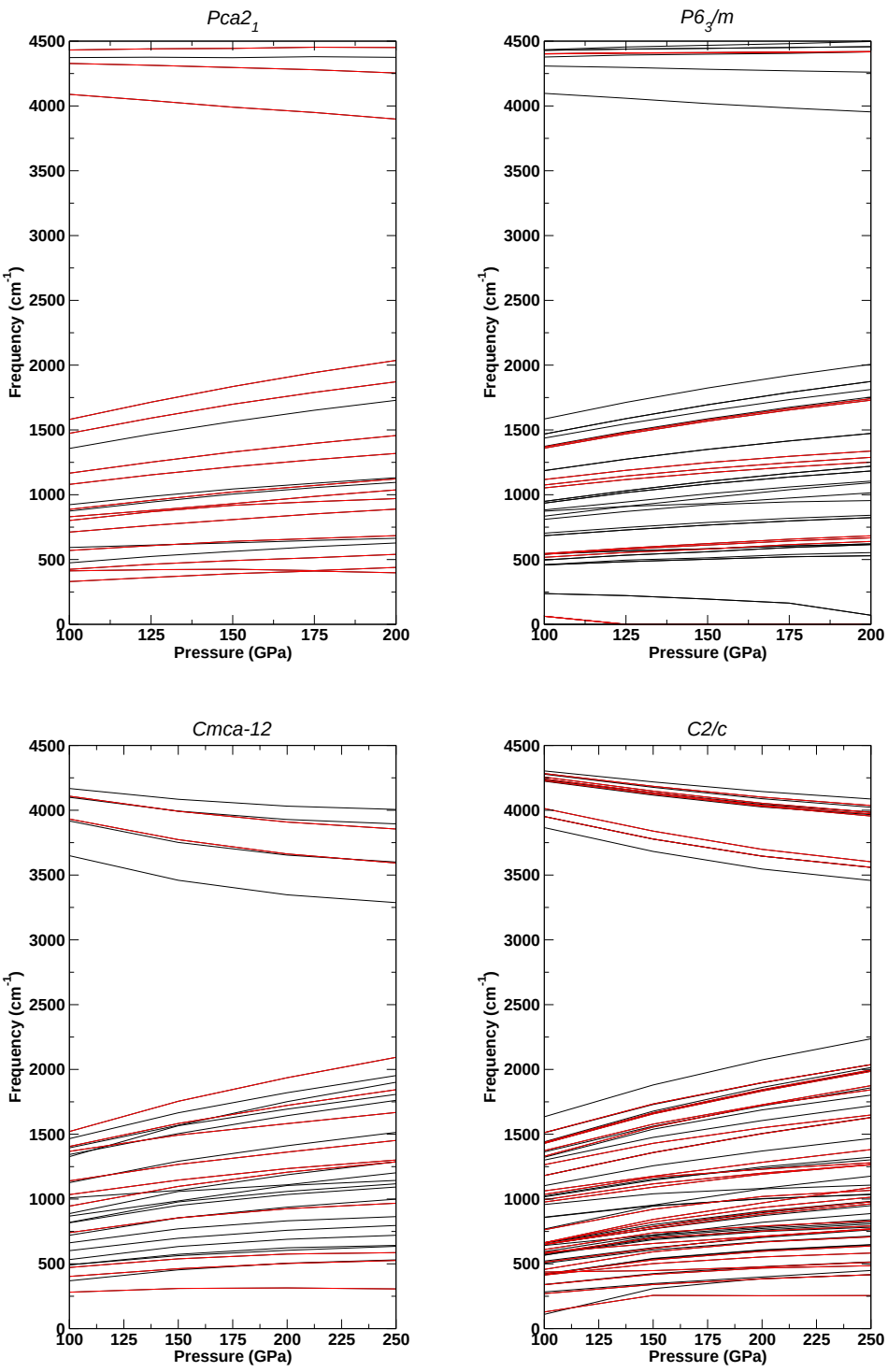

Figure 4: **Variation of the zone centre vibrational frequencies with pressure of the $Pca2_1$, $P6_3/m$, $Cmca$-12, and $C2/c$ structures.** The red lines indicate IR active modes (for clarity, intensities are not indicated) and the remaining modes are indicated by black lines.

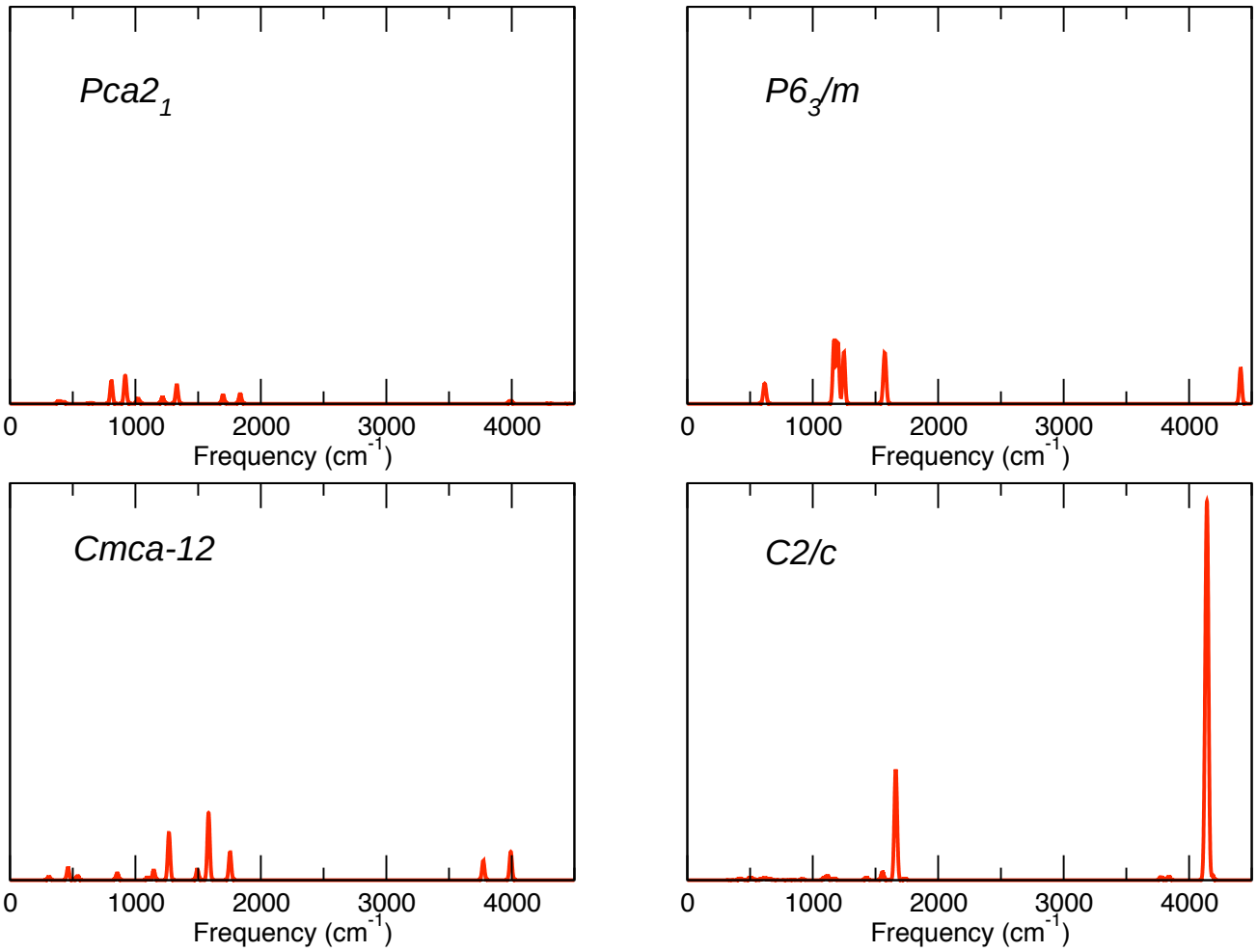

Figure 5: **Simulated IR spectra of the $Pca2_1$, $P6_3/m$, $Cmca$-12, and $C2/c$ structures at 150 GPa.** The spectra are broadened by a Gaussian of width 10 cm^{-1}, and the intensity scale is the same for all four structures.

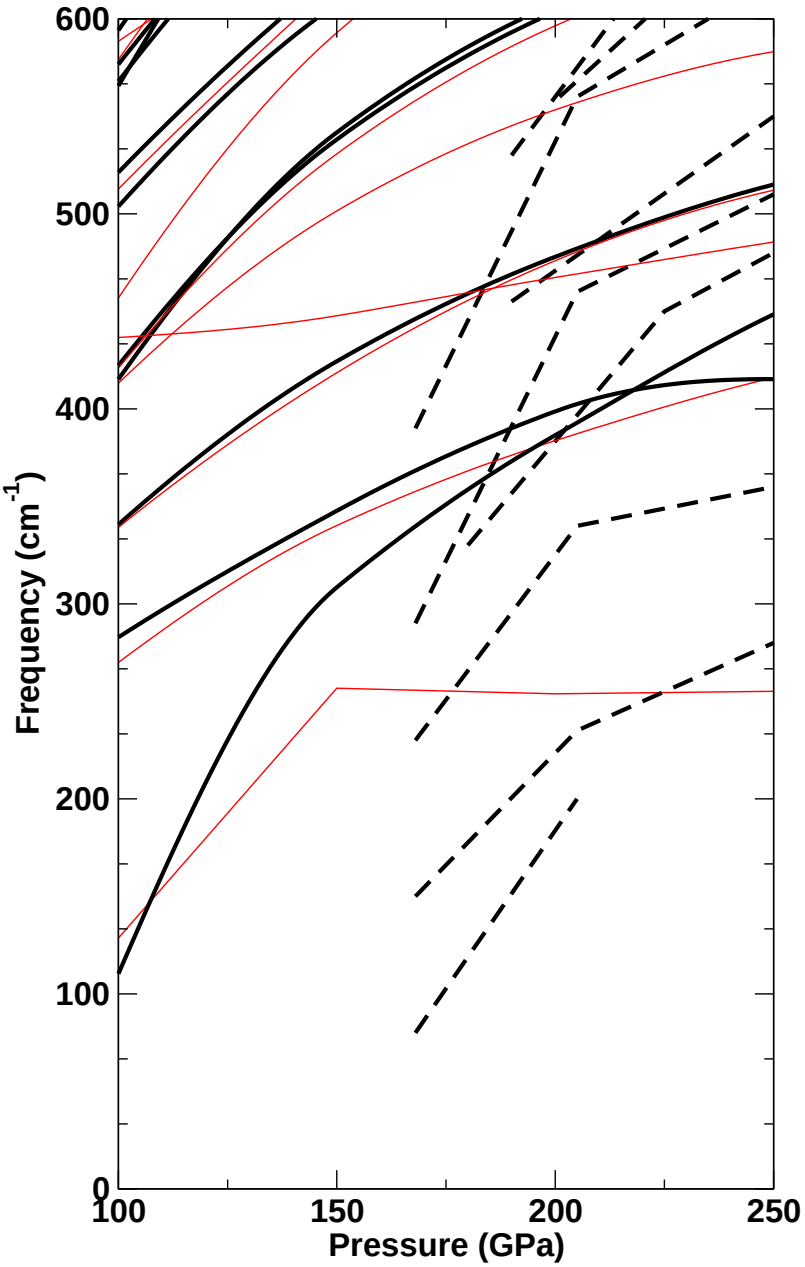

Figure 6: **Pressure dependence of the libron modes of $C2/c$ and of phase III.** The pressure dependence of the calculated vibrational frequencies of $C2/c$ (solid lines) compared with the experimental Raman data of Ref. 7 (dashed lines) in the low frequency libron region. The solid red lines indicate IR active modes.

Space group # atoms	Pressure (GPa)	Lattice parameters (Å, °)			Atomic coordinates (fractional)			
$P6_3/mmc$	100	a=1.881	b=1.881	c=3.032	H1	0.6667	0.3333	0.1281
4		α=90.00	β=90.00	γ=120.00				
$Pca2_1$	100	a=3.258	b=1.893	c=2.997	H1	0.3483	0.1296	0.3778
8		α=90.00	β=90.00	γ=90.00	H2	0.4855	0.3676	0.5011
$P2_1/c$	100	a=2.982	b=1.898	c=3.259	H1	0.2114	0.6542	0.0915
8		α=90.00	β=89.99	γ=90.00	H2	0.2896	0.3881	0.2391
$P6_3/m$	100	a=3.770	b=3.770	c=3.001	H1	0.0982	0.3903	0.2500
16		α=90.00	β=90.00	γ=120.00	H2	0.1984	0.2658	0.2500
					H3	0.3333	0.6667	0.6276
$C2/c$	300	a=4.939	b=2.811	c=4.139	H1	0.2260	0.0672	0.2464
12		α=90.00	β=142.47	γ=90.00	H2	0.3443	0.1958	0.2227
					H3	0.5000	0.1316	0.7500
					H4	0.5000	0.3988	0.7500
$B2/n$	300	a=2.838	b=5.024	c=4.906	H1	0.1851	0.1218	0.3144
24		α=90.00	β=90.00	γ=90.18	H2	0.0688	0.1110	0.4527
					H3	0.5336	0.1261	0.2232
					H4	0.6872	0.1245	0.3483
					H5	0.3787	0.1278	0.5871
					H6	0.6430	0.1387	0.5708

Table 1: **Structures of the phases.** The structures were optimised at the higher level of accuracy described in Section 1. Only the fractional coordinates of symmetry inequivalent atoms are reported. The numbers of atoms in a primitive cell are given. The $B2/n$ structure is the $C2/c$ structure described in the text, in a non-standard space group setting. The $C2/c$ structure in this table is a slightly less stable version, differing from the $B2/n$ structure only in its stacking.

Space group # atoms	Pressure (GPa)	Lattice parameters (Å, °)			Atomic coordinates (fractional)			
$Pbcn$	300	a=2.820	b=4.917	c=5.054	H1	0.4030	0.1132	0.0102
48		α=90.00	β=90.00	γ=90.00	H2	0.5859	0.2159	0.0158
					H3	0.5835	0.5554	0.0034
					H4	0.1473	0.1716	0.2495
					H5	0.3174	0.3416	0.2464
					H6	0.1693	0.4880	0.2506
$C2$	300	a=5.316	b=2.827	c=6.018	H1	0.0000	0.2330	0.0000
24		α=90.00	β=129.28	γ=90.00	H2	0.1648	0.0119	0.1598
					H3	0.3055	0.1560	0.3084
					H4	0.3387	0.5112	0.3382
					H5	0.1930	0.6573	0.1937
					H6	0.3020	0.4364	0.5378
					H7	0.3973	0.2452	0.6378
					H8	0.0000	0.5260	0.0000
					H9	0.6952	0.2595	0.9598
					H10	0.6077	0.4614	0.8672
					H11	0.5000	0.7361	0.5000
					H12	0.4401	0.9161	0.1886
					H13	0.5629	0.7781	0.3139
					H14	0.0000	0.5287	0.5000
$Ibam$	300	a=2.811	b=1.625	c=5.084	H1	0.4111	0.3386	0.0000
8		α=90.00	β=90.00	γ=90.00	H2	0.3332	0.0000	0.2500
$Cmca$	300	a=1.652	b=2.783	c=2.516	H1	0.0000	0.3696	0.4438
4		α=90.00	β=90.00	γ=90.00				
$Cmca$	300	a=2.555	b=4.748	c=2.871	H1	0.0000	0.0036	0.1358
12		α=90.00	β=90.00	γ=90.00	H2	0.0000	0.1317	0.4527
					H3	0.0000	0.2689	0.3163
high-$Cmca$	500	a=1.450	b=2.567	c=2.482	H1	0.0000	0.1132	0.1262
4		α=90.00	β=90.00	γ=90.00				

Table 2: **Structures of the phases.** The structures were optimised at the higher level of accuracy described in Section 1. Only the fractional coordinates of symmetry inequivalent atoms are reported. The numbers of atoms in a primitive cell are given.